Draft version September 5, 2016
Preprint typeset using LaTeX style AASTeX6 v. 1.0

arXiv:1609.00598v1 [physics.space-ph] 2 Sep 2016

SCALING OF COMPRESSIBLE MAGNETOHYDRODYNAMIC TURBULENCE IN THE FAST SOLAR WIND

S. Banerjee[1,2], L. Z. Hadid[2], F. Sahraoui[2], and S. Galtier[3]
[1] Universität zu Köln, Institut fur Geophysik und Meteorologie, Pohligstrasse 3, 50969 Köln, Germany

[2] LPP, CNRS-Ecole Polytechnique-UPMC-Université Paris-Sud, F-91128 Palaiseau, France
and
[3] LPP, Université Paris-Sud, Ecole Polytechnique, F-91128 Palaiseau, France

Abstract

The role of compressible fluctuations in the energy cascade of fast solar wind turbulence is studied using a reduced form of an exact law derived recently (Banerjee & Galtier 2013) for compressible isothermal magnetohydrodynamics and *in-situ* observations from the THEMIS B/ARTEMIS P1 spacecraft. A statistical survey of the data revealed a turbulent energy cascade over two decades of scales, which is broader than the previous estimates made from an exact incompressible law. A term-by-term analysis of the compressible model reveals new insight into the role played by the compressible fluctuations in the energy cascade. The compressible fluctuations are shown to amplify (2 to 4 times) the turbulent cascade rate with respect to the incompressible model in $\sim 10\%$ of the analyzed samples. This new estimated cascade rate is shown to provide the adequate energy dissipation required to account for the local heating of the non-adiabatic solar wind.

Keywords: heating — magnetohydrodynamics — plasma — solar wind — turbulence.

1. INTRODUCTION

The solar wind is an excellent natural laboratory for the *in situ* study of space plasma turbulence (Bruno & Carbone 2005; Galtier 2006). Due to the relatively weak density fluctuations ($\sim$ 10%), fast solar wind (FSW) turbulence is often described at low frequencies (< 0.1 Hz) by incompressible magnetohydrodynamics (MHD) (Goldstein & Roberts 1999; Sorriso-Valvo et al. 2007; Galtier 2012). However, the high correlation between the velocity and the magnetic field in the FSW leads to a strong imbalance between the outward and inward propagating Alfvén waves, which in turn makes the incompressible nonlinear cascade small. A compressible cascade may overcome this problem and explain the turbulent character of the FSW. Furthermore, it may provide a natural source for a local heating which is required in order to understand the slow decrease of the solar wind temperature with the heliospheric distance (Marsch et al. 1982; Vasquez et al. 2007). The pioneering works (Bavassano & Bruno 1989; Marsch & Tu 1990) included attempts to understand the origin and the nature of the density fluctuations, as well as their spectral laws. A Kolmogorov–like $-5/3$ spectrum for the density fluctuations led to the conclusion that the density acts as a passive scalar in the solar wind. However, in the following years, several studies explored the plausibility of an active participation of the density fluctuations using parametric decay of solar wind turbulence (Grappin et al. 2000; Malara et al. 2000). More recently, a study by Hnat, Chapman & Rowlands (2005) showed that the scaling of extended self-similarity of the density fluctuations does not coincide with that expected for a passive scalar (e.g., the magnetic field magnitude for incompressible MHD turbulence).

A direct evidence of the presence of an inertial energy cascade in the solar wind was observed using the so-called Yaglom law (Sorriso-Valvo et al. 2007; Marino et al. 2008). It is a universal law derived analytically from the incompressible MHD equations (Politano & Pouquet 1998) (hereafter PP98) under the assumptions of homogeneity, stationarity and isotropy of the turbulent fluctuations. Later, a first attempt was made to include the compressibility using a heuristic model (Carbone et al. 2009; Marino et al. 2011) (hereafter C09). The application of C09 to FSW turbulence showed a better scaling relation of the energy flux than with PP98. Furthermore, a significant increase of the turbulent cascade rate was evidenced and was shown to be sufficient to account for the local heating of the non-adiabatic solar wind expansion (Carbone et al. 2009). Although those results are original and constitute a real leap forward in studies of solar wind turbulence, (i) C09 remains a heuristic model (i.e., not derived analytically as the exact law of PP98), and gives a different origin of the amplification of the energy cascade rate than the one evidenced in the present work, (ii) following incompressible MHD tur-

biswayan@gmail.com

bulence, C09 attempted to verify two scaling relations corresponding to two pseudo-energy conservations, however, in compressible turbulence only the total energy is conserved (not the individual pseudo-energies) (Marsch & Mangeney 1987; Banerjee & Galtier 2013), and (iii) the frequency range chosen for the study does not seem to correspond fully to the MHD inertial range (Forman, Smith & Vasquez 2010; Sorriso-Valvo et al. 2010).

In this Letter, we present for the first time a statistical study of scaling properties of FSW turbulence using a reduced form of an exact law derived recently by Banerjee & Galtier (2013) (hereafter BG13) for compressible isothermal MHD turbulence (see also Galtier & Banerjee (2011)). Our findings show the new role played by the compressible fluctuations in the turbulent cascade and the local heating of the FSW.

2. DIFFERENT MODELS

In the course of this Letter, we shall compare two solar wind turbulent MHD models, namely the incompressible PP98 and the compressible isothermal BG13 exact laws. For the sake of clarity, we recall their different relationships written for the dissipation rate of the total energy. We recall that these laws are derived under the assumptions of a homogeneous, stationary turbulence, and in the asymptotic limit of large kinetic and magnetic Reynolds numbers.

INCOMPRESSIBLE MODEL: The PP98 law is written in terms of the Elsässer variables $\mathbf{z}^{\pm} = \mathbf{v} \pm \mathbf{v_A}$, where $\mathbf{v}$ is the flow velocity, $\mathbf{v_A} \equiv \mathbf{b}/\sqrt{\mu_0 \rho}$ is the magnetic field normalized to a velocity and ρ is the plasma density (in this incompressible model, we take $\rho = \langle \rho \rangle$). It reads (in the isotropic case)

$$-\frac{4}{3}\varepsilon_I \ell = \left\langle \frac{(\delta \mathbf{z}^+)^2}{2}\delta z_\ell^- + \frac{(\delta \mathbf{z}^-)^2}{2}\delta z_\ell^+ \right\rangle \langle \rho \rangle \equiv \mathcal{F}_I(\ell)\,, \tag{1}$$

where the general definition of an increment of a variable ψ is used, i.e. $\delta\psi \equiv \psi(\mathbf{x}+\boldsymbol{\ell}) - \psi(\mathbf{x})$. The longitudinal components are denoted by the index ℓ with $\ell \equiv |\boldsymbol{\ell}|$, $\langle\cdot\rangle$ stands for the statistical average and ε_I is the dissipation rate of the total energy. Note that in S.I. units, we have the relation $\langle \rho \rangle = 1.673 \times 10^{-21} \langle n_p \rangle$.

COMPRESSIBLE MODEL: The exact law BG13 can schematically be written as

$$-4\varepsilon_C = \nabla_{\boldsymbol{\ell}} \cdot \mathcal{F}_C - \Phi + \mathcal{S}\,, \tag{2}$$

where ε_C denotes the dissipation rate of the total compressible energy. The flux term writes

$$\mathcal{F}_C = \left\langle \tfrac{1}{2}\left[\delta(\rho \mathbf{z}^+)\cdot\delta\mathbf{z}^+\right]\delta\mathbf{z}^- + \tfrac{1}{2}\left[\delta(\rho\mathbf{z}^-)\cdot\delta\mathbf{z}^-\right]\delta\mathbf{z}^+ \right\rangle + \langle 2\delta\rho\delta e\delta\mathbf{v}\rangle + \left\langle 2\overline{\delta}\left(e + \tfrac{v_A^2}{2}\right)\delta(\rho_1\mathbf{v})\right\rangle\,, \tag{3}$$

where by definition $\overline{\delta}\psi \equiv (\psi(\mathbf{x}+\boldsymbol{\ell}) + \psi(\mathbf{x}))/2$ and e is the internal energy ($e = c_s^2 \ln(\rho/\langle\rho\rangle)$, with c_s the constant isothermal sound speed, $\langle\rho\rangle$ the mean density and $\rho = \langle\rho\rangle + \rho_1$). Note that $\mathcal{F}_C$ reduces to $\mathcal{F}_I$ when $\rho_1 = 0$ (implying also that $\delta\rho = 0$). Furthermore, we have

$$\Phi = \left\langle \frac{1}{\beta'}\nabla'\cdot(\rho\mathbf{v}e') + \frac{1}{\beta}\nabla\cdot(\rho'\mathbf{v}'e)\right\rangle\,, \tag{4}$$

where the primed and unprimed variables correspond to the variables at points $\mathbf{x}+\boldsymbol{\ell}$ and $\mathbf{x}$ respectively and $\beta = 2c_s^2/v_A^2$ gives the local ratio of thermal to magnetic pressure (note the difference between the definition of β used here and in Banerjee & Galtier (2013)). The last term $\mathcal{S}$ is a source term that includes the local divergences of $\mathbf{v}$ and $\mathbf{v_A}$. The main goal of this study is to evaluate for the first time the compressible effects in solar wind turbulence with an exact law. This objective will be partly achieved by evaluating the first two terms in the right hand side of Equation (2). The source term will be left aside because a reliable evaluation of local velocity divergences is not possible using single spacecraft data. Thus, we implicitly assume that $\mathcal{S}$ is subdominant. Note that this situation, not proved for the solar wind, is well observed numerically in supersonic HD turbulence (Kritsuk, Wagner & Norman 2013) and in a preliminary study using numerical simulations of isothermal MHD turblence (Servidio 2015).

We may try to estimate Φ, which is not a pure flux term but can be reduced to it, if the plasma β is relatively stationary. In this particular case, we obtain after simple manipulations

$$\Phi = \frac{1}{\beta}\nabla_{\boldsymbol{\ell}}\cdot\langle\rho\mathbf{v}e' - \rho'\mathbf{v}'e\rangle = -\frac{2}{\beta}\nabla_{\boldsymbol{\ell}}\cdot\left\langle\overline{\delta}e\delta(\rho\mathbf{v})\right\rangle\,. \tag{5}$$

This term can now be merged with the flux terms in Equation (3). This results in modifying the last term of $\mathcal{F}_C$ from $\overline{\delta}(e + v_A^2/2)\delta(\rho_1\mathbf{v})$ to $\overline{\delta}[(1+\beta^{-1})e + v_A^2/2]\delta(\rho_1\mathbf{v})$. As a last step, one can integrate relation (2) over a ball of radius ℓ and get the equivalent of the isotropic relation (1) for isothermal compressible MHD turbulence, namely

$$-\frac{4}{3}\varepsilon_C\ell = \mathcal{F}_{C+\Phi}(\ell)\,, \tag{6}$$

where

$$\mathcal{F}_{C+\Phi}(\ell) = \mathcal{F}_1(\ell) + \mathcal{F}_2(\ell) + \mathcal{F}_3(\ell)\,, \tag{7}$$

and

$$\mathcal{F}_1(\ell) = \left\langle \frac{1}{2}\left[\delta(\rho\mathbf{z}^-)\cdot\delta\mathbf{z}^-\right]\delta z_\ell^+ + \frac{1}{2}\left[\delta(\rho\mathbf{z}^+)\cdot\delta\mathbf{z}^+\right]\delta z_\ell^-\right\rangle\,,$$
$$\mathcal{F}_2(\ell) = \langle 2\delta\rho\delta e\delta v_\ell\rangle\,,$$
$$\mathcal{F}_3(\ell) = \left\langle 2\overline{\delta}\left[\left(1+\frac{1}{\beta}\right)e + \frac{v_A^2}{2}\right]\delta(\rho_1 v_\ell)\right\rangle\,. \tag{8}$$

Equations (6)–(8) will be evaluated using spacecraft data in the FSW. It is worth noting that the condition of uniform β used to obtain the new form of $\mathcal{F}_3(\ell)$ in Equations (8) is a stringent requirement in selecting the data used in the present study. We note however that it is the local β that is used in evaluting the flux terms and not its mean.

3. ESTIMATION OF THE ENERGY CASCADE RATES

3.1. *Data selection*

We used the THEMIS B/ARTEMIS P1 spacecraft data during time intervals when it was travelling in the free-streaming solar wind. In particular, we used the plasma moments and magnetic field data which were measured respectively by the Electrostatic Analyzer (ESA) and the Flux Gate Magnetometer (FGM) with a time resolution of 3 seconds (i.e., spin period). Since we are interested in FSW, we selected a total of 148 intervals between 2008 and 2011 for which $V_{sw} > 450\ \mathrm{km\,s^{-1}}$, where V_{sw} is the solar wind speed. Furthermore, we have tried as much as possible to avoid data intervals that contained significant ecliptic disturbances, such as coronal mass ejection or interplanetary shocks. Besides these criteria, we paid a particular attention to choosing only intervals that showed relatively stationary plasma β and $\Theta_{\mathbf{VB}}$, the angle between the local solar wind speed $\mathbf{V}$ and the magnetic field $\mathbf{B}$. The stationarity of the plasma β is imposed to fulfill the condition used to derive Equations (6)–(8), as discussed in the previous section. The stationarity of the angle $\Theta_{\mathbf{VB}}$ is required to guarantee that the spacecraft is sampling nearly the same direction of space with respect to the local magnetic field (when the Taylor hypothesis, $\ell \sim V\tau$, is used), which would ensure a better convergence in estimating the cascade rate. Indeed, if the angle $\Theta_{\mathbf{VB}}$ changes significantly in a single time interval (e.g., from $\sim 0°$ to $\sim 90°$), this means that the analysis would mix between the two cascade rates estimated along the direction parallel and perpendicular to the local magnetic field, known to be very different. This is based on anisotropic MHD turbulence models and on spacecraft observations in the solar wind (MacBride, Smith & Forman 2008) (this point will be discussed in more detail in an upcoming paper). The obtained intervals that fulfilled all the previous criteria were divided into a series of samples of equal duration $\sim$ 35mn, which corresponds to $\sim$ 700 data points with a 3s time resolution. This sample size is much larger than those used in previous studies based on ACE spacecract data that had a time resolution of 24s (e.g., MacBride, Smith & Forman (2008)). The sample size of 35mn ensures having at least one correlation time of the turbulent fluctuations estimated to vary in the range $\sim 20 - 30$mn. The data selection yielded 170 samples and a total number of data points $\sim 14 \times 10^4$. An example of the analyzed time intervals is shown in Figure 1. The average solar wind speed and plasma β for all the statistical samples are shown in Figure 2.

3.2. *Results*

We have constructed temporal structure functions of the different turbulent fields involved in the BG13 exact law at different time lags τ and verified their linear scaling with respect to τ. In order to probe into the scales of the inertial range, known to lie within the frequency range $\sim[10^{-4}, 1]$ Hz (based on the observation of the Kolmogorov-like $-5/3$ magnetic energy spectrum, Bruno & Carbone (2005); Marino et al. (2008)), we vary the time lag τ from 10 s to 1000 s thereby being well inside the targeted frequency range.

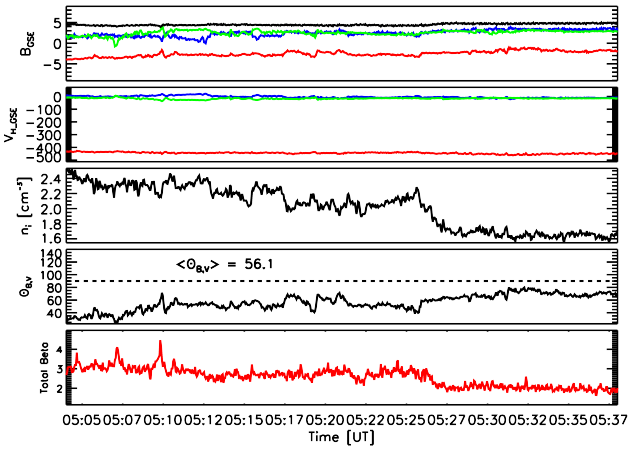

Figure 1. From top to bottom: the solar wind magnetic field components, ion velocity, ion number density, $\Theta_{\mathbf{VB}}$ angle and total plasma beta ($\beta = \beta_i + \beta_e$) measured by the FGM and ESA experiments onboard the THEMIS B spacecraft on day 2008-06-29 from 05:02 to 05:37.

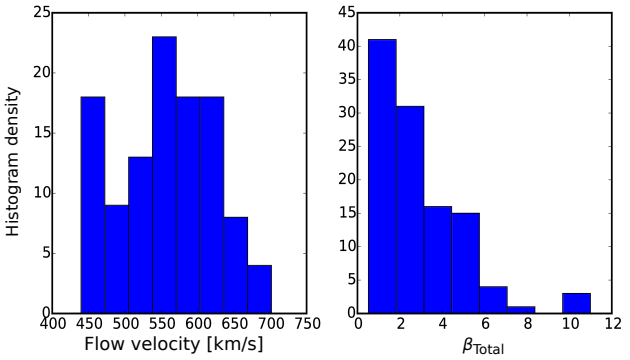

Figure 2. Histograms of the solar wind speed (left) and total plasma β (right) for all the statistical samples. Each sample represents 35mn ($\sim$ 700 points) of data.

Figure 3 (bottom) shows for a few case study (data from Fig. 1) a comparison between the energy cascade rates $\varepsilon_{I,C}$ of the incompressible and the compressible models. They were estimated using expressions (1) and (6). The compressibility, defined as $\sqrt{(\langle\rho^2\rangle - \langle\rho\rangle^2)}/\langle\rho\rangle$, is about 14%. One can see that the energy cascade rate from BG13 gives a smoother scaling than the PP98 model over two decades of (time) scales τ, which defines in a more rigorous way the size of the inertial range. This behaviour is representative of most of the other studied intervals, as can be seen from the few cases shown in the inset of Figure 3 (bottom). The value corresponding to the plateau gives an estimate of the rate of the total energy dissipation per unit volume (Vasquez et al. 2007; Marino et al. 2008). In the case of the isothermal compressible law, we obtain $|\varepsilon_C| \sim 6 \times 10^{-17}\mathrm{J\ m^{-3}s^{-1}}$. The estimate from the incompressible law gives a value

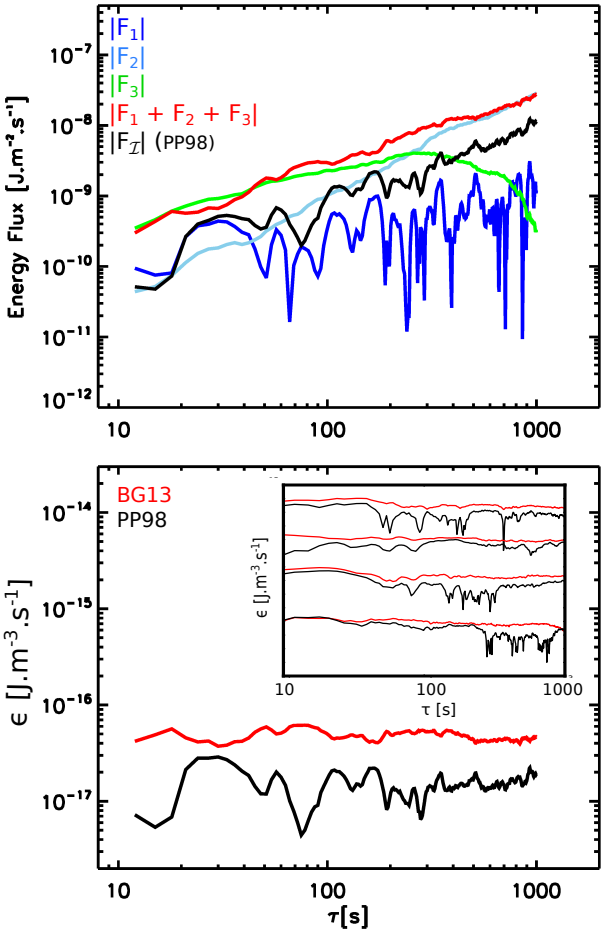

Figure 3. Top: comparison of the different terms $|\mathcal{F}_1|$, $|\mathcal{F}_2|$ and $|\mathcal{F}_3|$ (see text for the definitions) of the flux $\mathcal{F}_{C+\Phi}$. Bottom: comparison between the turbulent cascade rates given by the PP98 and BG13 models. The compressibility is 13.7%. The inset shows other examples for which BG13 model gives a smoother cascade rate over two decades than the PP98 model.

about 3 times smaller.

In order to quantify the contribution of the different compressible fluctuations, we show in Figure 3 (top) the different flux terms $\mathcal{F}_1$, $\mathcal{F}_2$ and $\mathcal{F}_3$ separately. Note that the flux $\mathcal{F}_1$ can be seen as the generalization to the compressible case of the PP98 flux since it converges to it in the incompressible limit. For that reason we call it the Yaglom flux. We clearly see that the main contribution comes from the new pure compressible fluxes $\mathcal{F}_2$ and $\mathcal{F}_3$ with up to an order of magnitude of difference with $\mathcal{F}_1$.

These results are confirmed in the statistical survey of all the samples. Figure 4 (right) compares the ratio between the estimated cascades rates from the PP98 and the BG13 models. It is interesting to note that, while the compressible and incompressible models converge toward the same value of the cascade rate for most of the events, some cases show that the compressible rate is a few times larger than the incompressible one. These ratios remain however smaller than those reported in Carbone et al. (2009) (this point will be discussed elsewhere). The absolute values of the compressible cascade

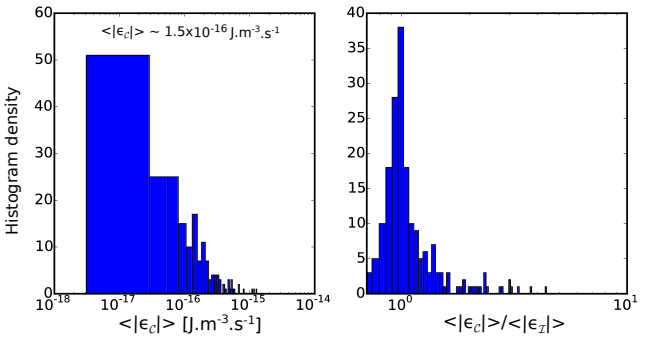

Figure 4. Left: histrogram of the average cascade rate for all the analyzed intervals. Right: histrogram of the ratio between the compressible (BG13) and incompressible (PP98) cascade rates.

rate ε_C (Fig. 4 – left) shows some spread around the mean value $\sim 1.5 \times 10^{-16}\,\mathrm{J\,m^{-3}\,s^{-1}}$.

More insight is gained when analyzing statistically the contribution of the different compressible fluxes, $\mathcal{F}_1$, $\mathcal{F}_2$ and $\mathcal{F}_3$, relative to the incompressible (Yaglom) flux $\mathcal{F}_I$. The result is shown in Figure 5. A first observation is that most of the samples have their compressible Yaglom flux ($\mathcal{F}_1$) of the order of the incompressible flux ($\mathcal{F}_I$). This confirms the previous result that the density fluctuations entering into the compressible Yaglom flux does not play a leading role in amplifying the compressible cascade rate w.r.t. the incompressible one. This role is rather played by the new compressible fluxes $\mathcal{F}_2$ and $\mathcal{F}_3$: high values of $\langle|\varepsilon_C|\rangle/\langle|\varepsilon_I|\rangle$ (up to ~ 4) are observed when $(\langle|\mathcal{F}_2|\rangle + \langle|\mathcal{F}_3|\rangle)/\langle|\mathcal{F}_I|\rangle > 1$. Although a similar amplification has been reported in Carbone et al. (2009), given by an heuristic modification of the incompressible (Yaglom) term *via* density fluctuations, the one observed here has a totally different origin: it is essentially due to the pure compressible terms $\mathcal{F}_2$ and $\mathcal{F}_3$ derived in the exact model of BG13. Note finally that the highest ratio $\langle|\varepsilon_C|\rangle/\langle|\varepsilon_I|\rangle$ (i.e., highest amplification of the cascade rate due to compressible fluctuations) is observed in the top-right quarter of Figure 5, which corresponds to the cases when all the three terms $\mathcal{F}_1$, $\mathcal{F}_2$ and $\mathcal{F}_3$ dominate over the incompressible (Yaglom) term $\mathcal{F}_I$.

4. DISCUSSION AND CONCLUSION

Unlike the incompressible PP98 model, the compressible flux obtained from BG13 model gives a uniform value of ε_C estimated above over two decades of scales, thereby assuring a physical cascade process in fast solar wind turbulence. Using the heuristic model, Carbone et al. (2009) found intervals for which either the inward or the outward flux scales linearly with the fluctuation scale. This problem has been overcome in the current study by using the flux of total energy which is an inviscid invariant of compressible MHD turbulence unlike the inward/outward flux separately.

The turbulent cascade implies a forward flux of energy which ultimately will be converted at small-scales into heating by some kinetic processes (see e.g. Sahraoui

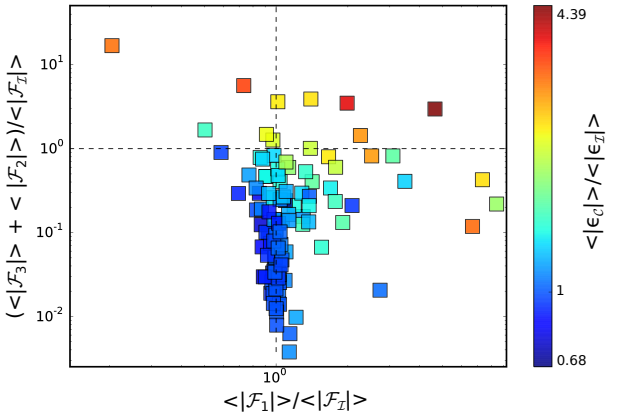

Figure 5. Estimation of the contribution of the compressible fluxes w.r.t. incompressible (Yaglom) flux to the total cascade rate.

et al. 2009, 2010). Using a simple power law model (Vasquez et al. 2007; Marino et al. 2008), we may obtain an estimate for the energy needed to heat up the fast solar wind at 1 AU. For a power-law of type $T(r) \sim r^{-\xi}$, with T the proton temperature and r the heliocentric distance, the model can be written as

$$\varepsilon_h = \frac{3}{2}\left(\frac{4}{3} - \xi\right)\frac{V_{sw} k_B T(r)}{m_p r}\,, \qquad (9)$$

where ε_h is the energy flux rate (per unit mass). Using the average flow velocity V_{sw} and temperature T for all the statistical events, with the value $\xi = 0.49$ (corresponding to the upper bound of the estimated temperature using Ulysses data (Marino et al. 2008)) we estimated $\epsilon_h = 2.7 \pm 1.9 \times 10^4 Jkg^{-1}s^{-1}$. This value is of the order of the estimated energy cascade rate from BG13 model, $\langle|\epsilon_C|\rangle = 1.5 \times 10^{-16} Jm^{-3}s^{-1} \sim 5.5 \times 10^4 Jkg^{-1}s^{-1}$ (using un average density $n_i = 1.7 \times 10^6 m^{-3}$), and also is in agreement with the finding of Carbone et al. (2009). However, unlike the current study, a considerably low incompressible flux ($\equiv 10$ times smaller than the compressible flux) is reported in Carbone et al. (2009) which can possibly be assigned to the absence of large scale drivers in the high latitude solar wind during solar minimum (MacBride, Smith & Forman 2008).

However, this model can be improved in the future by using polytropic closure (Banerjee & Galtier 2014), taking the non-homogeneity and the expansion of the wind into account (Verdini et al. 2015) and also considering the local anisotropy of the turbulence which is known to be important (Matthaeus, Goldstein & Roberts 1990; Stawarz et al. 2009; Narita et al. 2010; Sahraoui et al. 2010; Osman et al. 2011; Galtier 2012). Previous studies (MacBride, Smith & Forman 2008) have indeed shown that the heating is smaller in the parallel direction than in the perpendicular one, the latter being comparable however to the isotropic heating. A simple observational approach to account for anistropy would be to examine the dependence of the compressible cascade rate on the angle $\Theta_{\mathbf{VB}}$. A more complete approach would consist in splitting into two parts the flux term in Equation (2) by assuming cylindrical isotropy around the local mean magnetic field direction. These problems will be investigated in a forthcoming paper where a detailed study of the nature of the cascade (direct *vs* inverse, inward *vs* outward) and a comparison between the fast and slow solar winds will be made (Hadid et al., in preparation).

ACKNOWLEDGMENT. The THEMIS/ARTEMIS data come from the AMDA data base (http://amda.cdpp.eu/). We are grateful to Dr. O. Le Contel and Dr. L. Sorriso Valvo for useful discussions. FS acknowledges financial support from the ANR project THESOW, grant ANR-11-JS56-0008. The french participation in the THEMIS/ARTEMIS mission is funded by CNES and CNRS.

REFERENCES

Banerjee, S., & Galtier, S. 2013, Phys. Rev. E, 87, 013019
Banerjee, S., & Galtier, S. 2014, J. Fluid Mech., 742, 230
Bavassano, B., & Bruno, R. 1989, J. Geophys. Res., 94, 11977
Bruno, R., & Carbone, V. 2005, Living Rev. Solar Phys., 2, 4
Carbone, V., Marino, R., Sorriso-Valvo, L., et al. 2009, Phys. Rev. Lett., 103, 061102
Forman, M. A., Smith, C. W., & Vasquez, B. J. 2010, Phys. Rev. Lett., 104, 189001
Galtier, S. 2006, J. Low Temp. Phys., 145, 59
Galtier, S., & Banerjee, S. 2011, Phys. Rev. Lett., 107, 134501
Galtier, S. 2012, Astrophys. J., 746, 184
Grappin, R., Mangeney, A., & Marsch, E. 1990, J. Geophys. Res., 95, 8197
Goldstein, M. L., & Roberts, D. A. 1999, Phys. Plasmas, 6, 4154
Hnat, B., Chapman, S. C., & Rowlands, G. 2005, Phys. Rev. Lett., 94, 204502
Kritsuk, A. G., Wagner, R., & Norman, M. L. 2013, J. Fluid Mech., 729, R1
MacBride, B., Smith, C. W., & Forman, M. 2008, Astrophys. J., 679, 1644
Malara, F., Primavera, L., & Veltri, P., 2000, Phys. Plasmas, 7, 2866
Marino, R., Sorriso-Valvo, L., Carbone, V. et al. 2008, Astrophys. J. Lett., 677, L71
Marino, R., Sorriso-Valvo, L., Carbone, V., et al. 2011, Planet. Space Sci., 59, 592
Marsch, E., Schwenn, R., Rosenbauer, H., et al. 1982, J. geophys. Res., 87, 52
Marsch, E, & Mangeney, A. 1987, J. Geophys. Res., 92, 7363
Marsch, E., & Tu, C.-Y. 1990, J. Geophys. Res., 95, 11945
Matthaeus, W. H., Goldstein, M. L., & Roberts, D. A. 1990, J. Geophys. Res., 95, 20673
Narita, Y., Glassmeier, K.-H., Sahraoui, F., et al. 2010, Phys. Rev. Lett., 104, 171101
Osman, K. T., Wan, M., Matthaeus, W. H., et al. 2011, Phys. Rev. Lett., 107, 165001
Politano, H., & Pouquet, A. 1998, Phys. Rev. E, 57, 21

Sahraoui, F., Goldstein, M. L., Robert, P., et al. 2009, Phys. Rev. Lett., 102, 231102

Sahraoui, F., Goldstein, M. L., Belmont, G., et al. 2010, Phys. Rev. Lett., 105, 131101

Servidio, S. 2015, Private Communication

Sorriso-Valvo, L., Marino, R., Carbone, V., et al. 2007, Phys. Rev. Lett., 99, 115001

Sorriso-Valvo, L., Carbone, V., Marino, R., et al. 2010, Phys. Rev. Lett., 104, 189002

Stawarz, J. E., Smith, C. W., Vasquez, B. J., et al. 2009, Astrophys. J., 697, 1119

Vasquez, B., Smith, C. W., Hamilton, K., et al. 2007, J. Geophys. Res., 112, 7101

Verdini, A., Grappin, R., Hellinger, P., et al. 2015, Astrophys. J., 804, 119